HER2 kinase domain mutation results in constitutive phosphorylation and activation of HER2 and EGFR and resistance to EGFR tyrosine kinase inhibitors

Shizhen Emily Wang,[1] Archana Narasanna,[2] Marianela Perez-Torres,[1] Bin Xiang,[5] Frederick Y. Wu,[2] Seungchan Yang,[2] Graham Carpenter,[3] Adi F. Gazdar,[6] Senthil K. Muthuswamy,[5] and Carlos L. Arteaga[1,2,4,*]

[1] Department of Cancer Biology, Vanderbilt University School of Medicine, Nashville, Tennessee 37232
[2] Department of Medicine, Vanderbilt University School of Medicine, Nashville, Tennessee 37232
[3] Department of Biochemistry, Vanderbilt University School of Medicine, Nashville, Tennessee 37232
[4] Breast Cancer Research Program, Vanderbilt-Ingram Comprehensive Cancer Center, Vanderbilt University School of Medicine, Nashville, Tennessee 37232
[5] Cold Spring Harbor Laboratory, Cold Spring Harbor, New York 11724
[6] Hamon Center for Therapeutic Oncology Research, University of Texas Southwest Medical Center, Dallas, Texas 75390
*Correspondence: carlos.arteaga@vanderbilt.edu

Summary

***HER2/Neu* gene mutations have been identified in lung cancer. Expression of a HER2 mutant containing a G776^{YVMA} insertion in exon 20 was more potent than wild-type HER2 in associating with and activating signal transducers, phosphorylating EGFR, and inducing survival, invasiveness, and tumorigenicity. HER2^{YVMA} transphosphorylated kinase-dead EGFR^{K721R} and EGFR^{WT} in the presence of EGFR tyrosine kinase inhibitors (TKIs). Knockdown of mutant HER2 in H1781 lung cancer cells increased apoptosis and restored sensitivity to EGFR TKIs. The HER2 inhibitors lapatinib, trastuzumab, and CI-1033 inhibited growth of H1781 cells and cells expressing exogenous HER2^{YVMA}. These data suggest that (1) HER2^{YVMA} activates cellular substrates more potently than HER2^{WT}; and (2) cancer cells expressing this mutation remain sensitive to HER2-targeted therapies but insensitive to EGFR TKIs.**

Introduction

HER2/Neu (ErbB2) is a member of the ErbB family of transmembrane receptor tyrosine kinases, which also includes the epidermal growth factor receptor (EGFR, ErbB1), HER3 (ErbB3), and HER4 (ErbB4). Binding of ligands to the ectodomain of EGFR, ErbB3, and ErbB4 results in the formation of catalytically active homo- and heterodimers to which HER2 is recruited as a preferred partner (Yarden and Sliwkowski, 2001). Although HER2 cannot bind any of the ErbB ligands directly, its catalytic activity can potently amplify signaling by ErbB-containing heterodimers via increasing ligand binding affinity and/or receptor recycling and stability (Graus-Porta et al., 1997; Pinkas-Kramarski et al., 1996; Wang et al., 1998; Worthylake et al., 1999). Activation of the ErbB network leads to receptor autophosphorylation in C-terminal tyrosines and the recruitment to these sites of cytoplasmic signal transducers that regulate cellular processes such as proliferation, differentiation, motility, adhesion, protection from apoptosis, and transformation. Cytoplasmic signal transducers that are activated by this network include PLC-γ1, Ras-Raf-MEK-MAPKs, phosphatidylinositol-3 kinase (PI3K)-Akt-ribosomal S6 kinase, Src, the stress-activated protein kinases (SAPKs), PAK-JNKK-JNK, and the signal transducers and activators of transcription (STATs) (Yarden and Sliwkowski, 2001).

HER2 gene amplification has been reported in approximately 20% of metastatic breast cancers, where it is associated with poor patient outcome (Slamon et al., 1989). Trastuzumab, a humanized monoclonal IgG_1 that binds the extracellular domain of HER2, has been shown to induce clinical responses in HER2-overexpressing breast cancers and prolong patient survival (Slamon et al., 2001; Vogel et al., 2002). HER2 is overexpressed

SIGNIFICANCE

Mutations in the kinase domain of the *HER2/Neu* proto-oncogene were identified recently. Expression of a HER2 mutant containing a G776^{YVMA} insertion in exon 20 was more potent than wild-type HER2 in activating postreceptor signal transducers and in transforming mammary and bronchial epithelial cells. HER2^{YVMA} activated the EGFR in the presence of EGFR tyrosine kinase inhibitors (TKIs). Knockdown of mutant HER2 in H1781 lung cancer cells induced cell death and sensitized these cells to EGFR TKIs. The HER2 inhibitors lapatinib, trastuzumab, and CI-1033 inhibited growth of cells expressing mutant HER2. These data suggest that (1) HER2^{YVMA} signals more potently than HER2^{WT}; and (2) cancer cells harboring exon 20 insertions in HER2 remain sensitive to HER2-targeted therapies but insensitive to EGFR TKIs.

in a cohort of non-small cell lung cancers (NSCLCs), and increased *HER2* gene copy number has been associated with therapeutic response to EGFR tyrosine kinase inhibitors (TKIs) (Cappuzzo et al., 2005; Hirsch et al., 2002). Recently, intragenic somatic mutations in the *HER2* gene were reported in <5% of NSCLCs. These involve in-frame duplications/insertions in a small stretch within exon 20 that correspond to the identical nine codon region in exon 20 of the *EGFR* gene, where duplications/insertions have also been reported (Stephens et al., 2004). Interestingly, mutations in both receptor genes do not overlap and occur predominantly in patients of Asian ethnicity, nonsmokers, females, and lung adenocarcinomas (Shigematsu et al., 2005). Because of the location of these insertions at the C-terminal end of the αC helix in the tyrosine kinase domain, it has been postulated that they result in a conformational change and shift in the helical axis, thus narrowing the ATP binding cleft and increasing kinase activity over that in wild-type receptors (Gazdar et al., 2004).

To study the potential gain-of-function effects of *HER2* mutations, we generated a retroviral vector encoding HER2 with an in-frame YVMA insertion at residue 776, which is the most common abnormality detected in a recent survey in 96 unselected NSCLC specimens (Shigematsu et al., 2005). Stable expression of $HER2^{YVMA}$ in BEAS2B bronchial and MCF10A mammary epithelial cells resulted in enhanced transformation compared to cells transduced with wild-type HER2. $HER2^{YVMA}$ was potently autophosphorylated and induced transphosphorylation of kinase-dead EGFR and HER3 as well as higher association with signal transducers that activate proliferative and antiapoptotic pathways compared to $HER2^{WT}$. RNA interference of mutant but not wild-type HER2 in a lung cancer cell line containing a VC insertion at G776 in exon 20 inhibited antiapoptotic signals and induced tumor cell death. Cells expressing $HER2^{YVMA}$ or $HER2^{VC}$ exhibited resistance to the EGFR TKIs such as erlotinib and gefitinib but remained sensitive to direct HER2 inhibitors such as the receptor antibody trastuzumab and the small molecule dual kinase inhibitors lapatinib and CI-1033.

Results

Transient and stable expression of $HER2^{YVMA}$ mutant

We generated a retroviral vector encoding Myc-tagged full-length $HER2^{YVMA}$ (Figure S1A in the Supplemental Data available with this article online). Vectors expressing wild-type HER2 ($HER2^{WT}$) and $HER2^{YVMA}$ were transiently transfected into 293 human embryonic kidney cells. Cells expressing $HER2^{YVMA}$ contained higher levels of phosphorylated MAPK and Akt compared to vector- or $HER2^{WT}$-transfected cells (Figure S1B, lanes 1–3). In immunoblots of Myc pull-downs, $HER2^{YVMA}$ showed higher tyrosine phosphorylation and stronger associations with the adaptor proteins Shc and p85 compared to $HER2^{WT}$ (Figure S1B, lanes 4–6).

Human immortalized BEAS2B bronchial and MCF10A mammary epithelial cells were then stably transduced with $HER2^{YVMA}$ or $HER2^{WT}$ retroviral vectors. After single colony selection, transgene expression was detected by Myc and HER2 immunoblot. In both lines, $HER2^{YVMA}$-transfected clones exhibited higher levels of a tyrosine phosphorylated protein that comigrated with the HER2 and Myc bands compared to clones expressing $HER2^{WT}$ (Figures S1C and S1D). BEAS2B and MCF10A clones expressing equal levels of $HER2^{WT}$ and $HER2^{YVMA}$ were selected for subsequent functional studies.

$HER2^{YVMA}$ is more transforming than $HER2^{WT}$ in bronchial epithelial cells

We next determined the transforming effects of $HER2^{YVMA}$ on bronchial epithelial cells. BEAS2B cells expressing $HER2^{YVMA}$ proliferated faster than cells expressing $HER2^{WT}$ or empty vector in both serum-containing and serum-free medium (Figure 1A). Cell survival was assessed by Apo-BrdU assay. After serum starvation for 3 days, 16%–18% of the BEAS2B cells expressing $HER2^{WT}$ or vector exhibited evidence of apoptosis as measured by the incorporation of Br-dUTP into double-stranded DNA. However, expression of $HER2^{YVMA}$ protected the cells from apoptosis induced by serum starvation (Figure 1B). Similar results were obtained in anchorage-independent colony-forming assays. Ten days after seeding in soft agar, cells expressing $HER2^{YVMA}$ formed 40% more and significantly larger colonies than $HER2^{WT}$-expressing cells (Figure 1C). To determine if increased focus formation correlated with tumorigenicity in vivo, cells were injected in athymic nude mice. Ten days after s.c. inoculation, four out of six mice injected with cells expressing $HER2^{YVMA}$ exhibited established tumors, whereas no tumor was detected in animals injected with cells expressing $HER2^{WT}$ or vector alone (Figure 1D). Finally, we examined the effect of the HER2 insertion mutation on cell motility. $HER2^{YVMA}$-expressing cells migrated into the wounded area and closed the wound within 24 hr, whereas in BEAS2B/$HER2^{WT}$ cells the wound remained open. Similar results were obtained in transwell assays, where cells expressing the insertion mutant exhibited 3-fold increased migration through 5 μm pore size filters (Figure 1E).

$HER2^{YVMA}$ is a more potent suppressor of apoptosis than $HER2^{WT}$ in mammary epithelial cells

The transforming effects of ectopic $HER2^{WT}$ have been well characterized in MCF10A human mammary epithelial cells (Debnath and Brugge, 2005). In these cells, endogenous HER2 protein levels are undetectable (Figure S1D). Compared to the modest proliferative effect of transfected $HER2^{WT}$ over vector controls, stable expression of $HER2^{YVMA}$ resulted in accelerated anchorage-dependent growth (Figure 2A). MCF10A cells form polarized, quiescent acini-like spheroids in three-dimensional (3D) basement membrane gels. Activation of chimeric ErbB2 in these cells reinitiates proliferation, disrupts tight junctions and apical polarity, and induces acinar expansion but without invasion into the surrounding matrix. MCF10A cells expressing $HER2^{WT}$ or $HER2^{YVMA}$ were grown on Matrigel containing basement membrane components. As early as day 4, $HER2^{YVMA}$-expressing cells formed multiacinar structures that by day 14 exhibited invading protrusions into the surrounding matrix. This process was more delayed with MCF10A/$HER2^{WT}$ cells, which developed into smaller multiacinar structures with a hollow lumen (Figure 2B, days 14–16, arrows). Acini were trypsinized and cell numbers were determined at regular intervals. MCF10A/$HER2^{YVMA}$ cells continued to proliferate up to 16 days, whereas the slower proliferation of $HER2^{WT}$ cells reached a plateau after day 10 (Figure 2C). The large multiacinar structures formed by $HER2^{YVMA}$-expressing cells suggested a more invasive phenotype. Therefore, we examined the ability of the cells to invade through Matrigel-coated chambers. Cells were seeded on top of a Matrigel invasion chamber and allowed to

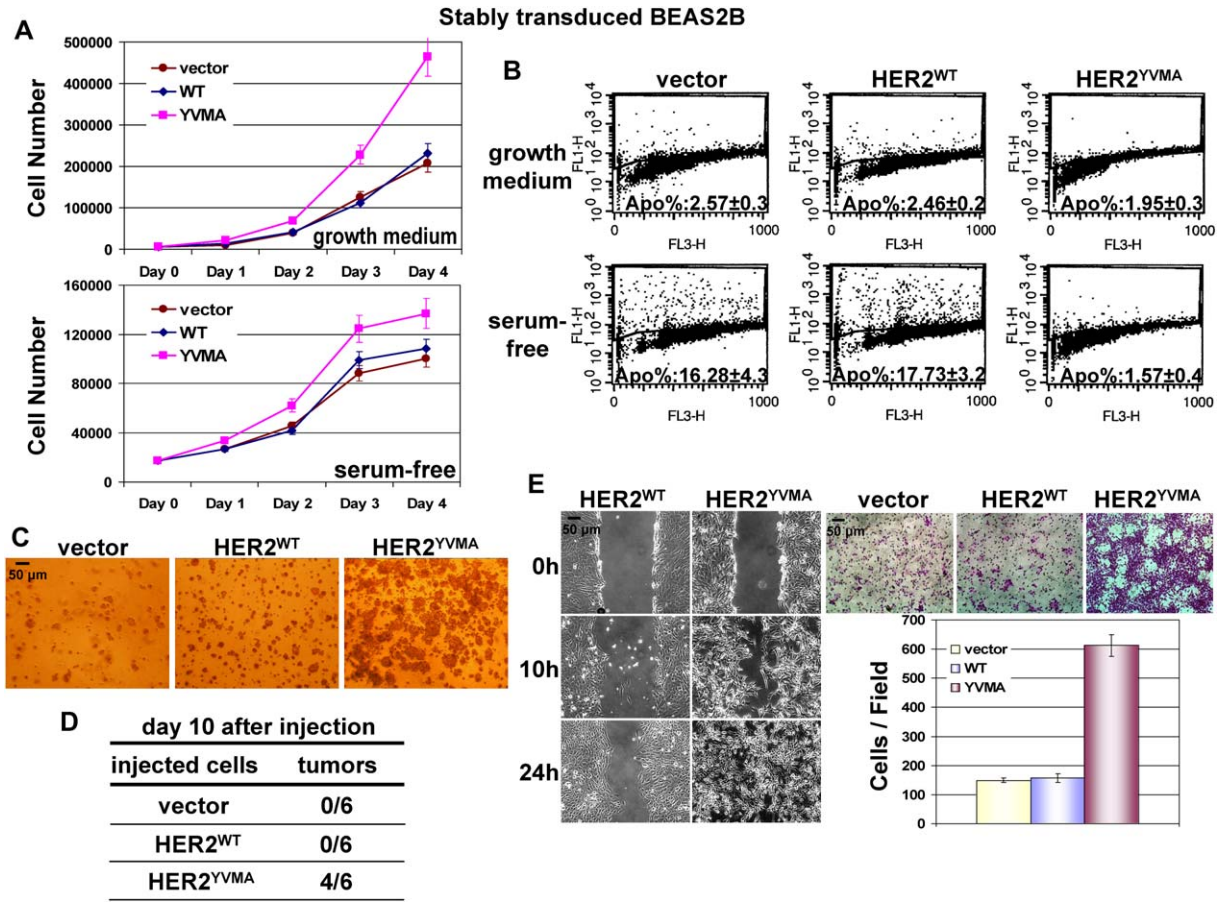

Figure 1. HER2^{YVMA} is potently transforming in bronchial epithelial cells

A: BEAS2B cells stably expressing HER2^{WT}, HER2^{YVMA}, or vector were seeded on 12-well plates and allowed to grow in full growth medium or serum-free medium. Cells were trypsinized and counted every 24 hr. Each data point represents the mean ± SD of four wells.

B: Stably transduced BEAS2B cells were maintained in growth medium or serum starved for 3 days before being subjected to Apo-BrdU assay as described in Experimental Procedures. The percentage of FITC+ (apoptotic) cells is indicated. Quantitative data represent the mean ± SD of three experiments.

C: Stably transduced BEAS2B cells were seeded in colony-forming assay as described in Experimental Procedures. Colonies were photographed at day 10.

D: The indicated BEAS2B cells (2×10^6) were injected s.c. in athymic nude mice. Detectable tumors of ≥3 mm in minimal diameter are shown (n = 6 per group).

E: Left panel: close-to-confluent monolayers of BEAS2B cells in serum-free medium were wounded with a pipette tip; wound closure was monitored at the indicated times. Right panel: transwell assays. Cells that had migrated to the underside of transwell filters are shown after fixation. Quantitative data are depicted below, with each bar representing the mean ± SD of six fields from three independent experiments.

invade into it for 24 hr. Compared to controls, HER2^{WT} and HER2^{YVMA} cells invaded 3-fold and 10-fold more the other side of the Matrigel chamber, respectively (Figure 2D).

In cell survival assays, both MCF10A/HER2^{WT} and vector control cells exhibited 58%–62% apoptosis after 3 days of serum starvation, whereas cells expressing the insertion mutant were protected from apoptosis (Figure 2E). Cells in the center of MCF10A polarized acini grown in 3D have been shown to undergo apoptosis resulting in the formation of a central lumen. Apoptosis and lumen formation have been shown to be prevented by the expression of activated oncogenes (Debnath et al., 2002). Thus, we subjected MCF10A acini to immunofluorescence staining of cleaved (active) caspase-3, an apoptosis marker, and Ki-67, a proliferation marker. In day 8 HER2^{WT} acini, the centrally located cells underwent apoptosis, as indicated by caspase-3 staining. However, caspase-3 was undetectable in HER2^{YVMA} acini (Figure 2F). In day 14 HER2^{WT} acini, Ki-67 staining was mostly located at the edges, whereas in HER2^{YVMA}-expressing acini, both peripheral and centrally located cells were proliferating (Ki-67+; Figure 2G).

HER2^{YVMA} kinase has stronger catalytic activity than HER2^{WT}

ErbB receptor chimeras containing the ligand binding domain of FK506 binding protein (FKBP) can be induced to homodimerize by the bivalent ligand AP1510 and, therefore, provide a method to elucidate the activity of ectopic ErbB homo- and heterodimers without interference from the endogenous ErbB receptors (Muthuswamy et al., 1999). Thus, we constructed HER2 chimeras containing the extracellular and transmembrane domains of low-affinity NGF receptor (p75), the kinase domain (aa 676–1255) of HER2^{YVMA} or HER2^{WT}, and two copies of FKBP with an HA tag at the carboxyl terminus. MCF10A cells stably expressing equal levels of the two chimeras were treated with AP1510 to induce receptor homodimerization. In cells expressing the wild-type chimera, HER2^{WT} phosphorylation was modestly induced by AP1510. However, in cells expressing the mutant chimera, HER2^{YVMA} phosphorylation was high in the absence of AP1510 and induced further by the addition of the dimerizing ligand (Figure 3A).

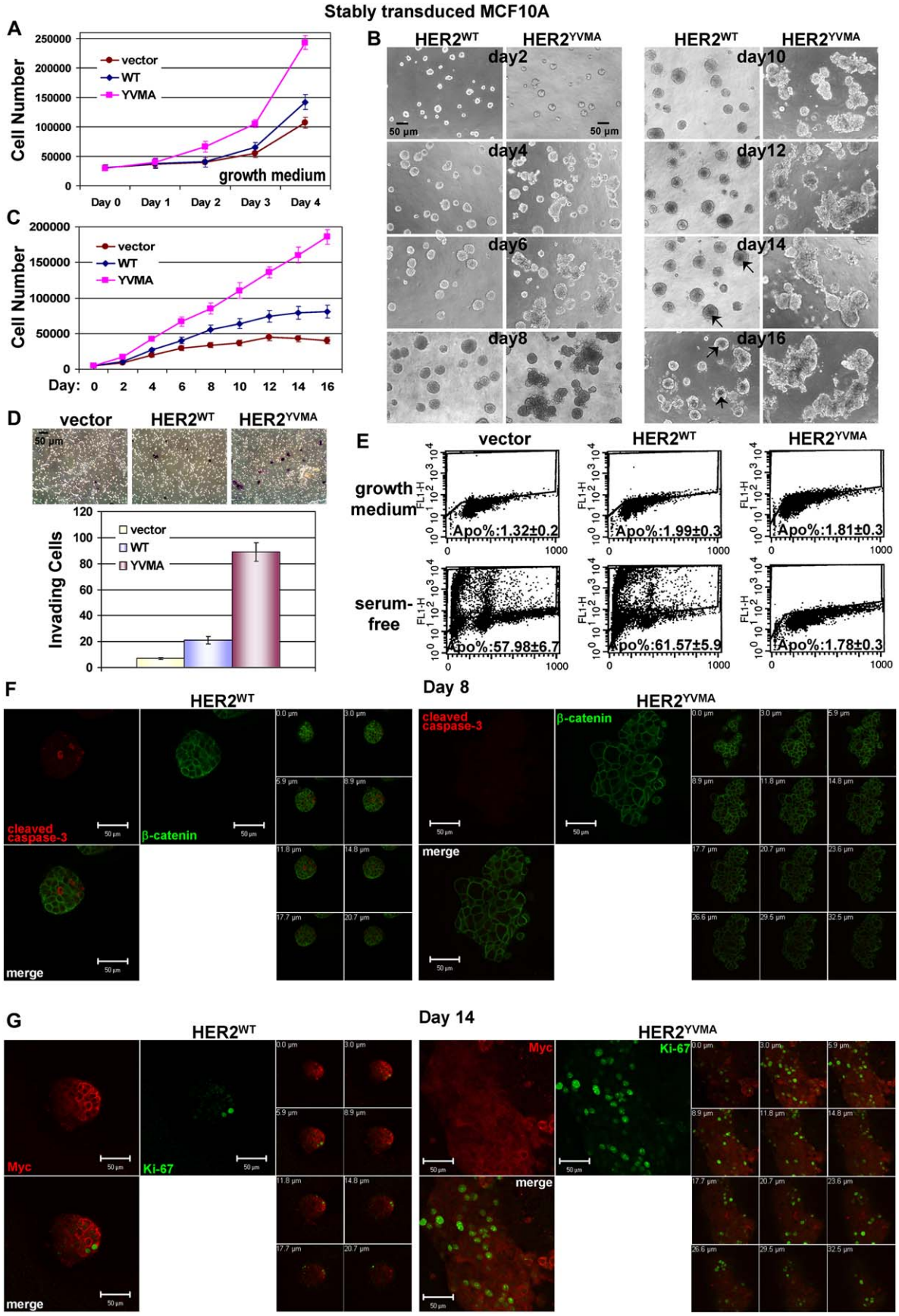
Stably transduced MCF10A
A
Cell Number
vector
WT
YVMA
growth medium
Day 0
Day 1
Day 2
Day 3
Day 4
B
HER2WT
HER2YVMA
day2
day4
day6
day8
day10
day12
day14
day16
50 μm
C
Cell Number
Day:
D
vector
HER2WT
HER2YVMA
Invading Cells
E
growth medium
serum-free
Apo%:1.32±0.2
Apo%:1.99±0.3
Apo%:1.81±0.3
Apo%:57.98±6.7
Apo%:61.57±5.9
Apo%:1.78±0.3
F
Day 8
cleaved caspase-3
β-catenin
merge
G
Day 14
Myc
Ki-67
merge

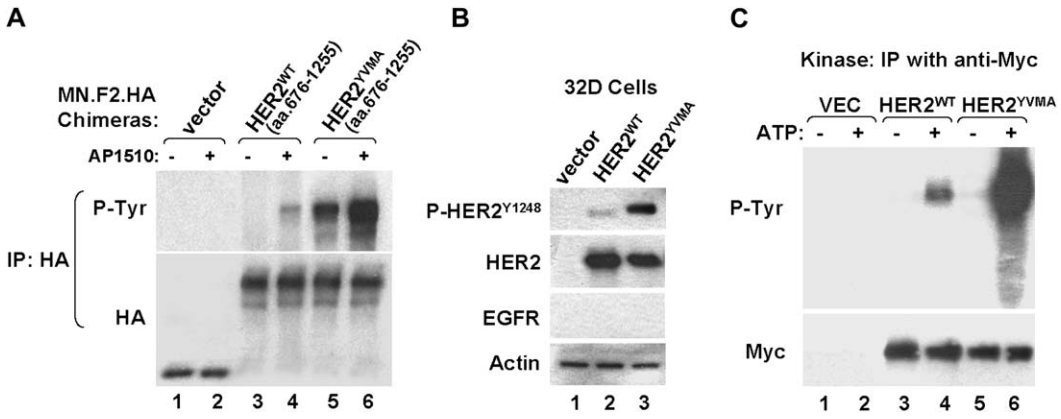

Figure 3. HER2^{YVMA} has a more potent kinase activity compared to HER2^{WT}

A: MCF10A cells stably expressing HER2^{WT} or HER2^{YVMA} chimeras or empty vector were serum starved for 24 hr before treatment with 1 μM AP1510 for 15 min. Cell lysates were precipitated with an HA antibody; the HA pull-downs were subjected to P-Tyr and HA immunoblot analysis as indicated in Experimental Procedures.

B: 32D cells stably expressing full-length HER2^{WT}, HER2^{YVMA}, or vector control were serum starved for 4 hr, lysed, and subjected to the indicated immunoblot analyses.

C: HER2^{WT} or HER2^{YVMA} receptors expressed in MCF10A cells were precipitated with a Myc antibody. An in vitro kinase assay was performed as described in Experimental Procedures, and the products were analyzed by 7.5% SDS-PAGE followed by P-Tyr and Myc immunoblots.

In 32D murine hematopoietic cells that do not express endogenous ErbB receptors or ligands (Pierce et al., 1988), expression of equal levels of the full-length receptors also showed a higher constitutive phosphorylation of HER2^{YVMA} compared to HER2^{WT} using an antibody that recognizes HER2 phosphorylated at Y1248 (DiGiovanna and Stern, 1995) (Figure 3B). Increased autophosphorylation of HER2^{YVMA} could result from either increased receptor homodimerization (Figure 3A) and/or a more potent kinase activity. To further test this second possibility, Myc-tagged wild-type and mutant HER2 were precipitated from MCF10A/HER2^{WT} and MCF10A/HER2^{YVMA} cells, respectively, and the pull-downs were tested in an in vitro kinase reaction. When ATP was added, HER2^{YVMA} showed markedly higher tyrosine phosphorylation than HER2^{WT} (Figure 3C), suggesting that the insertion mutant has higher autocatalytic activity. Similar results were obtained with wild-type and mutant HER2 precipitated from 32D cells (data not shown).

HER2^{YVMA} associates with and activates the EGFR in the absence of ErbB ligands and EGFR kinase activity

We next examined the ability of HER2^{YVMA} to associate with and activate exogenous substrates. To minimize ligand-induced receptor activity, cells were serum starved 24 hr prior to experimental manipulation. In both BEAS2B and MCF10A cells stably transduced with HER2^{YVMA}, HER2^{WT}, or vector alone, the levels of EGFR, Shc, p85, MAPK (ERK), and Akt were the same. However, basal levels of Y1068 P-EGFR, Y416 P-Src, P-Akt, and P-MAPK were markedly higher in HER2^{YVMA} compared to HER2^{WT} cells (Figure 4A, lanes 1–6). To determine the activation status of ectopic HER2, Myc pull-downs were tested by P-Tyr and Y1248 P-HER2 immunoblots. Y1248 P-HER2 was only detected in the Myc precipitate from HER2^{YVMA}-expressing cells. A much stronger P-Tyr band coprecipitated with Myc in these cells compared with HER2^{WT}-expressing cells. The fainter P-Tyr band in HER2^{WT} cells, where Y1248 P-HER2 was not detected in the Myc precipitates, suggests that HER2 is phosphorylated in tyrosines other than Y1248 in MCF10A/HER2^{WT} cells. Finally, higher levels of EGFR, Y1068 P-EGFR, Shc, and p85 coprecipitated with Myc in cells expressing the insertion mutant compared to HER2^{WT} cells (Figure 4A, lanes 7–12). Higher levels of Y1289 P-HER3 and increased HER3:HER2 association were observed in HER2^{YVMA}-expressing MCF10A cells but not in BEAS2B cells, probably as a result of the lower levels of HER3 in the latter cells (Figure 4A).

In BEAS2B/HER2^{WT} cells, TGFα stimulated anchorage-dependent growth (Figure S2A), EGFR (Y1068) and HER2 (Y1248) phosphorylation, and activation of Akt and MAPK (Figure S2B, lanes 1–4). Conversely, the addition of TGFα did

Figure 2. HER2^{YVMA} induces a gain of function over HER2^{WT} in mammary epithelial cells

A: MCF10A cells seeded on 12-well plates in full growth medium were trypsinized and counted every 24 hr. Each data point represents the mean ± SD of four wells.

B: Phase contrast images of HER2^{WT}- or HER2^{YVMA}-expressing MCF10A acini cultured on basement membrane in 8-well chambers and followed every 2 days. Scale bars, 50 μm.

C: MCF10A acini (from **B**) were trypsinized and counted every 48 hr. Each data point represents the mean ± SD of four wells.

D: Stably transduced MCF10A cells were seeded at 2.5 × 10^4 cells/well on Matrigel-coated transwells and allowed to invade toward growth medium. At 24 hr invading cells were counted; each bar represents the mean ± SD of three wells.

E: MCF10A cells were maintained in growth medium or serum starved for 3 days before being subjected to Apo-BrdU assay as described in Experimental Procedures. The mean percentage ± SD of FITC+ apoptotic cells from three wells is indicated.

F: MCF10A cells expressing HER2^{WT} or HER2^{YVMA} were cultured on basement membrane for 8 days and stained with antibodies against β-catenin (green) and cleaved caspase-3 (red).

G: Transduced MCF10A cells were cultured on basement membrane for 14 days and stained with Ki-67 (green) and Myc tag (red) antibodies. Scale bars, 50 μm. In both panels, serial confocal sections of the stained acini were photographed at 2.96 μm intervals.

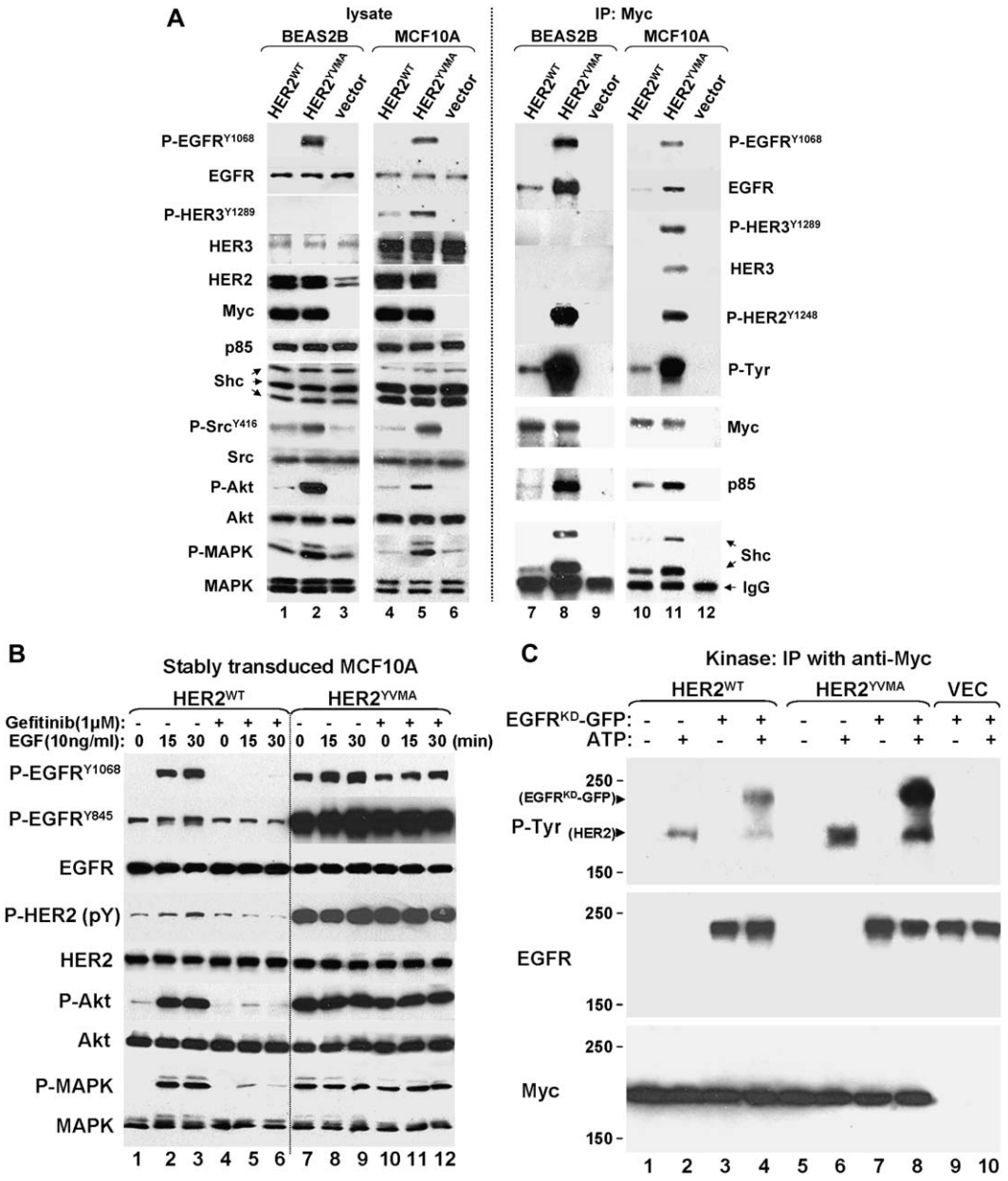

Figure 4. HER2^{YVMA} induces ligand-independent EGFR phosphorylation, which does not require the EGFR tyrosine kinase

A: BEAS2B and MCF10A cells expressing HER2^{WT}, HER2^{YVMA}, and vector were serum starved for 24 hr, lysed, and then subjected to SDS-PAGE or precipitation with a Myc tag antibody. Total cell lysates (left) and Myc pull-downs were tested by immunoblots with the indicated antibodies.

B: MCF10A cells were serum starved for 24 hr and treated with 10 ng/ml EGF. At 0–30 min, the monolayers were lysed and the cell lysates subjected to the indicated immunoblot analyses. For P-HER2, lysates were immunoprecipitated with HER2 antibody followed by immunoblot with P-Tyr monoclonal antibody. Where indicated, 1 μM gefitinib was added 4 hr prior to EGF.

C: HER2^{WT} or HER2^{YVMA} receptors expressed in MCF10A cells were precipitated with a Myc antibody. EGFR^{K721R} (EGFR^{KD})-GFP expressed in 32D cells was pulled down with a GFP antibody. An in vitro kinase assay was performed as described in Experimental Procedures, and the products were analyzed by 7.5% SDS-PAGE followed by P-Tyr, Myc, and EGFR immunoblot analyses. The molecular weights (in kDa) are shown at the left of the gel. Positions of EGFR^{KD}-GFP and HER2 receptors are indicated by arrows.

not increase the high basal phosphorylation of EGFR, HER2, Akt, and MAPK in cells expressing HER2^{YVMA} (Figure S2B, lanes 5–8), nor did it stimulate monolayer growth (Figure S2A). Similar results were observed in MCF10A cells. Treatment with EGF potently induced Y1068 EGFR, HER2, MAPK, and Akt phosphorylation in MCF10A/HER2^{WT}. However, in HER2^{YVMA}-expressing cells, EGF only modestly increased the high basal P-HER2 and EGFR phosphorylation at Y1068 and Y845 (Figure 4B). Further, recombinant EGF stimulated proliferation and migration in MCF10A cells expressing HER2^{WT} but had no effect in cells expressing HER2^{YVMA} (Figures S2C and S2D).

In cells expressing HER2^{WT}, ligand-induced Y1068 P-EGFR, P-HER2, P-MAPK, and P-Akt were efficiently blocked by the EGFR small molecule TKI gefitinib. However, gefitinib had little or no effect on EGFR, HER2, MAPK, and Akt phosphorylation in MCF10A/HER2^{YVMA} cells in the presence or absence of

added ligand. In both cell types, gefitinib did not block EGFR phosphorylation at Y845 (Figure 4B). Phosphorylation of this residue does not depend on EGFR tyrosine kinase activity (Stover et al., 1995) and has been shown to be induced by c-Src (Biscardi et al., 1999), consistent with the higher levels of P-Src in cells expressing $HER2^{YVMA}$ (Figure 4A). The results with gefitinib suggested that the EGFR/HER2 association and EGFR phosphorylation in cells expressing $HER2^{YVMA}$ did not require EGFR's catalytic activity. Therefore, we performed an in vitro kinase assay using GFP-fused K721R (kinase-dead) EGFR (Ewald et al., 2003) ($EGFR^{KD}$) as substrate. Myc-tagged wild-type and mutant HER2 receptors were precipitated from transfected MCF10A cells and incubated with $EGFR^{KD}$-GFP in the presence or absence of ATP. In the absence of ATP, no phosphorylation of $EGFR^{KD}$-GFP was detected. Both $HER2^{WT}$ and $HER2^{YVMA}$ phosphorylated $EGFR^{KD}$-GFP in vitro, but this effect was at least 5-fold higher with the insertion mutant (Figure 4C).

Cells expressing $HER2^{YVMA}$ are resistant to EGFR inhibitors but still sensitive to HER2 inhibitors

The EGFR TKIs erlotinib and gefitinib inhibited the weak basal EGFR phosphorylation in MCF10A/$HER2^{WT}$ cells (Figure 5A, lanes 1–11). Although not direct inhibitors of HER2, it has been shown that (EGFR-specific) low concentrations of erlotinib or gefitinib inhibit HER2 phosphorylation and growth of HER2-dependent tumor cells, presumably by blocking the EGFR tyrosine kinase and, thus, interfering with EGFR-HER2 crosstalk and heterodimerization (Hernan et al., 2003; Moasser et al., 2001; Moulder et al., 2001). Consistent with this, erlotinib and gefitinib suppressed $HER2^{WT}$ cell proliferation in a dose-dependent manner (Figure S3, top) and inhibited the 3D growth of these acini in Matrigel devoid of added EGFR ligands (Figure 5C, top). On the other hand, the ability of $HER2^{YVMA}$ to transactivate the EGFR in an EGFR kinase-independent manner anticipated lack of an inhibitory effect of EGFR TKIs against cells expressing the insertion mutant. Indeed, erlotinib and gefitinib had no effect on EGFR and HER2 phosphorylation in MCF10A/$HER2^{YVMA}$ cells (Figure 5A, lanes 15–25) nor inhibited their growth in monolayer (Figure S3, bottom) or in 3D in Matrigel (Figure 5C, bottom).

We next examined the effect of direct inhibitors of HER2 on the insertion mutant. Treatment with the HER2 antibody trastuzumab downregulated both wild-type and mutant receptors from the cell surface, as indicated by HER2 immunoblot of streptavidin precipitates of surface-biotinylated cells (Figure 5B). However, treatment with trastuzumab inhibited growth and invasiveness of $HER2^{YVMA}$ but not $HER2^{WT}$ acini in 3D. This lack of an effect of trastuzumab on cells overexpressing $HER2^{WT}$ is consistent with the reported inability of the IgG_1 to interfere with EGF, TGFα, and heregulin-induced growth and/or EGFR/HER2 heterodimerization (Agus et al., 2002; Moulder et al., 2001; Ye et al., 1999). The EGFR/HER2 dual TKI lapatinib (Rusnak et al., 2001) inhibited EGFR and HER2 phosphorylation in MCF10A/$HER2^{WT}$ cells (Figure 5A, lanes 12–14). Lapatinib also inhibited $HER2^{YVMA}$ and EGFR phosphorylation in $HER2^{YVMA}$ cells but at higher concentrations (Figure 5A, lanes 26–28). Trastuzumab alone or in combination with lapatinib also suppressed Y1068 P-EGFR (Figure S4). The growth in 3D of $HER2^{YVMA}$-expressing acini was also suppressed by lapatinib, although not as much as with MCF10A/$HER2^{WT}$ acini (Figure 5C). The combination of lapatinib and trastuzumab was the most potent in suppressing growth of $HER2^{YVMA}$ acini (Figure 5C). Addition of erlotinib or gefitinib did not enhance the effect of trastuzumab against these cells (data not shown). At day 8 and day 14, $HER2^{YVMA}$ acini treated with both drugs exhibited apoptotic cells in the center, similar to those exhibited by $HER2^{WT}$ acini (Figure 5D, compared to Figures 2F and 2G). These data suggest that $HER2^{YVMA}$ is still sensitive to direct inhibitors of HER2.

Mutant HER2 in H1781 cells is required for proliferation and survival

NCI-H1781 lung cancer cells express wild-type EGFR and contain a VC insertion at G776 in exon 20 of the *HER2* gene (Shigematsu et al., 2005) (Figure S1A). Small interfering RNA oligonucleotides targeting $HER2^{WT}$, $HER2^{MUT}$, or a control sequence were transfected into H1781 cells. Three days posttransfection, we used a PCR primer set specific for mutant HER2 mRNA and observed efficient knockdown of $HER2^{MUT}$ in cells expressing siRNA targeting $HER2^{MUT}$ but not $HER2^{WT}$. The *HER2* mutation in H1781 cells has been reported to be homozygous (Shigematsu et al., 2005), explaining the lack of $HER2^{WT}$ mRNA expression by RT-PCR (Figure 6A). By immunoblot analysis, RNAi resulted in 90% reduction of mutant HER2 protein as well as basal P-MAPK and P-Akt (Figure 6B). These cells exhibited markedly increased apoptosis (by cleaved caspase-3 staining) and decreased proliferation (by Ki-67 staining), compared to cells transfected with siRNA targeting $HER2^{WT}$ or the control sequence (Figure 6C). Similar to MCF10A/$HER2^{YVMA}$ cells, trastuzumab, lapatinib, and the combination, but not erlotinib and gefitinib, inhibited H1781 colony formation (Figure 6D). In cells expressing siRNA targeting $HER2^{MUT}$ but not in control cells, erlotinib and gefitinib reduced H1781 colony formation (Figure 6D), suggesting that the insertion mutant counteracts the inhibitory effect of the EGFR TKIs.

The irreversible ErbB2 inhibitor CI-1033 is a potent inhibitor of the mutant HER2

It has been shown that a mutant EGFR with an exon 20 insertion is resistant to gefitinib and erlotinib but highly sensitive to the irreversible covalent EGFR/HER2 inhibitor CL-387,785 (Greulich et al., 2005). Therefore, we tested the effect of a similar irreversible inhibitor, the 4-anilinoquinazoline CI-1033, which is predicted to covalently modify Cys773 within the ATP binding site of the HER2 kinase (Citri et al., 2002; Smaill et al., 2000). In dose-dependent fashion, submicromolar concentrations of CI-1033 inhibited tyrosine phosphorylation of wild-type and mutant HER2 and EGFR in transfected MCF10A and H1781 cells (Figure 7A). The same range of concentrations (0.1–3 μM) markedly inhibited growth on Matrigel of both MCF10A/$HER2^{WT}$ and MCF10A/$HER2^{YVMA}$ cells, but the dose response was steeper against cells expressing the mutant (Figure 7B). Similar concentrations of CI-1033 also inhibited H1781 colony formation in soft agar with a 25% and 90% reduction in colony number at 0.1 and 1 μM, respectively (Figure 7C).

Discussion

The orphan HER2/Neu (ErbB2) receptor plays a critical role in the cellular responses mediated by ligand-dependent activation of ErbB coreceptors (Yarden and Sliwkowski, 2001). Indeed, overexpression of Neu alone or in combination with EGFR or HER3 can transform mammary epithelial cells and fibroblasts (Pierce et al., 1991; Zhang et al., 1996). Transgenic mice

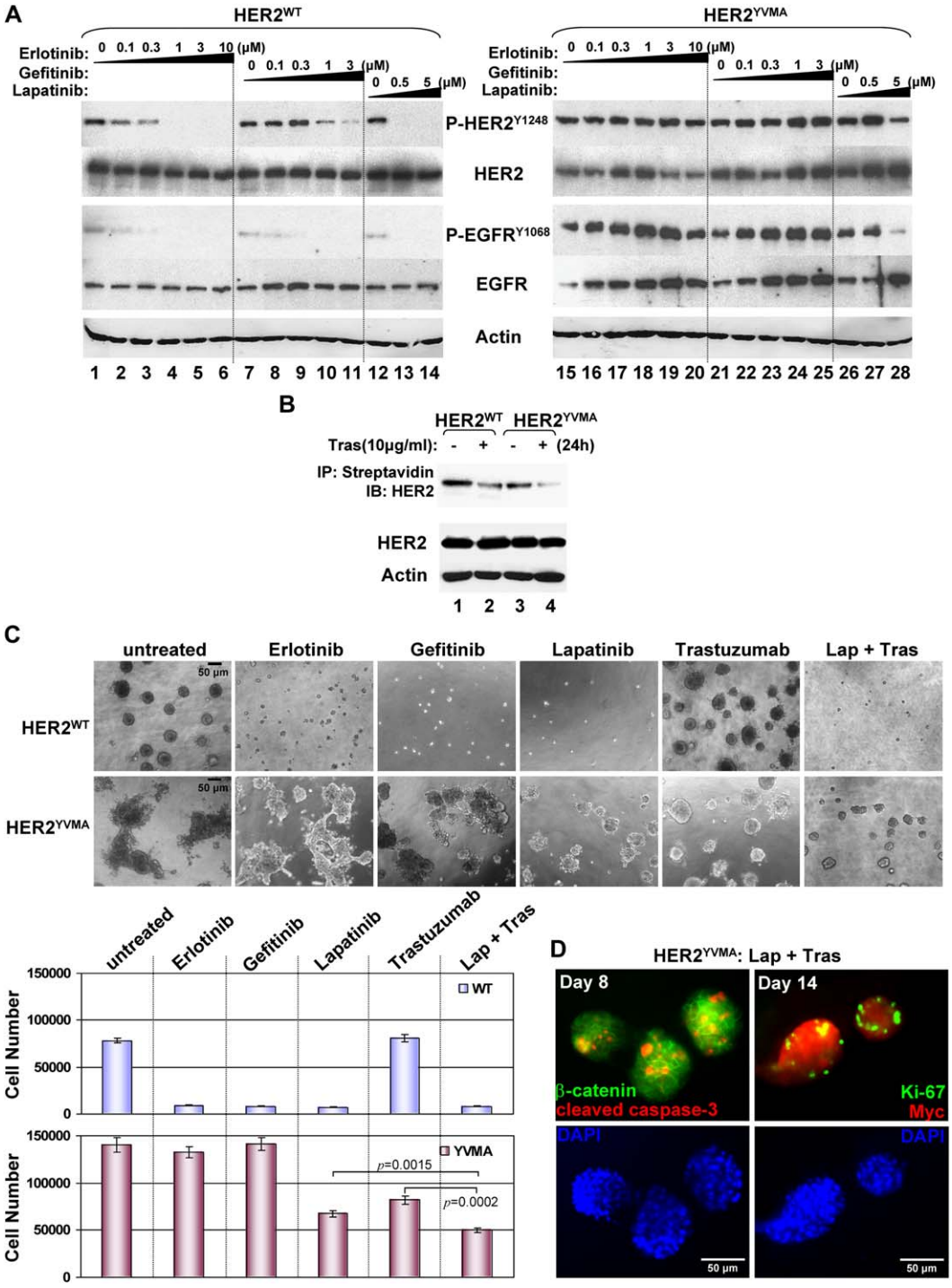

Figure 5. EGFR inhibitors are inactive against cells expressing HER2^{YVMA}

A: MCF10A cells expressing HER2^{WT} or HER2^{YVMA} were treated for 24 hr with erlotinib, gefitinib, or lapatinib at the indicated concentrations. Cell lysates were prepared, separated by SDS-PAGE, and subjected to immunoblots using the indicated antibodies.

B: Cells were treated with trastuzumab (10 μg/ml) followed by acid wash to remove bound antibody. Cell surface proteins were then biotinylated at 4ºC as indicated in Experimental Procedures. Cell lysates were precipitated with Streptavidin Magnetic Spheres followed by HER2 immunoblot. To control for gel loading, whole-cell lysates were subjected to HER2 and actin immunoblots (bottom panels).

C: Top: HER2^{WT}- or HER2^{YVMA}-expressing MCF10A cells were plated on basement membrane in 8-well chambers with or without erlotinib (3 μM), gefitinib (1 μM), lapatinib (5 μM), trastuzumab (10 μg/ml), or the combination of lapatinib and trastuzumab as indicated in Experimental Procedures. Inhibitors were replenished every 2 days. The phase contrast image shown was recorded 12 days after the initial seeding of cells. Scale bars, 50 μm. Bottom: 12-day acini were trypsinized, and total cell number was determined in a Coulter counter. Each bar graph represents the mean ± SD of four wells. p values were calculated using Student's t test.

D: At day 8 and day 14, HER2^{YVMA} acini treated with the combination of lapatinib and trastuzumab were stained for β-catenin (green) and cleaved caspase-3 (red) (day 8), or Ki-67 (green) and Myc tag (red) (day 14). DAPI (blue), nuclear staining. Scale bars, 50 μm.

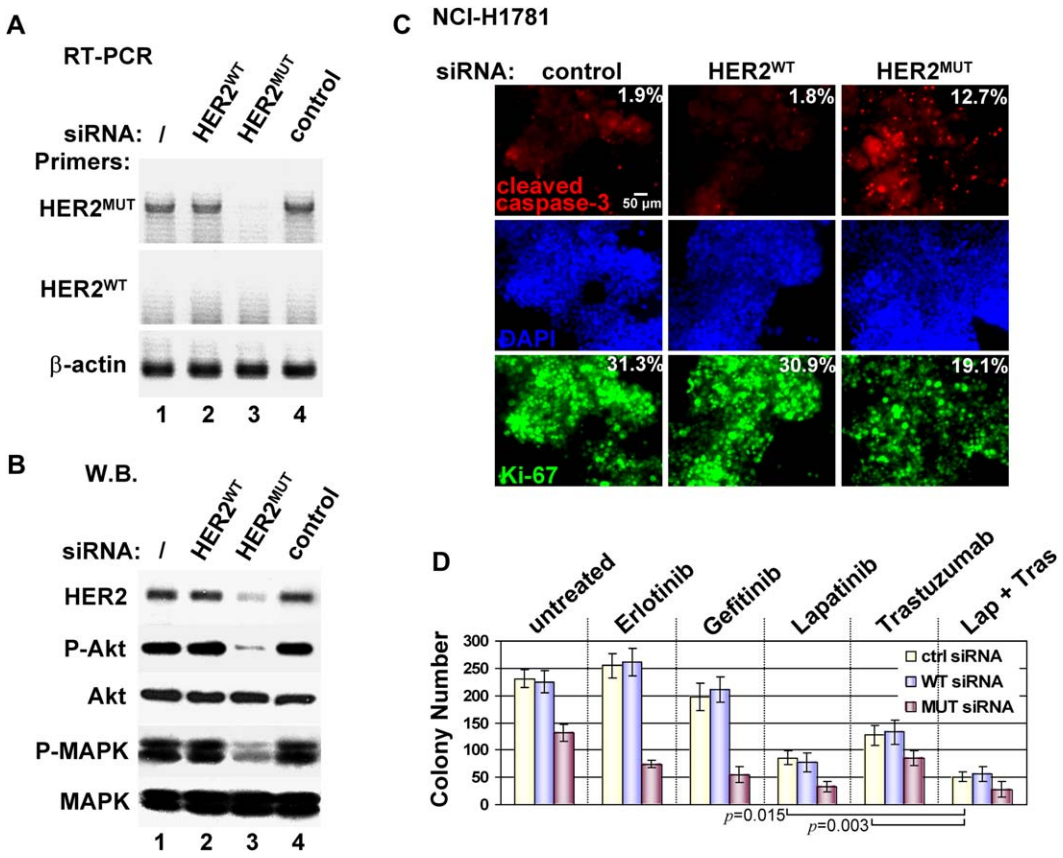

Figure 6. RNA interference of mutant HER2 inhibits survival of H1781 lung cancer cells

A: H1781 cells grown on 6-well plates were transfected by siRNA oligonucleotides targeting $HER2^{WT}$, $HER2^{MUT}$, or a control sequence. At day 3 after transfection, total RNA was extracted. Two hundred nanograms of RNA were used in the RT-PCR reaction as described in Experimental Procedures. Gene-specific primer pairs were used to amplify $HER2^{MUT}$, $HER2^{WT}$, and β-actin cDNA (control). ''/'' lane indicates mock-transfected cells.

B: H1781 cells were lysed 3 days after transfection and analyzed by immunoblot using the indicated antibodies.

C: H1781 cells growing on glass coverslips were transfected by specific siRNA. At day 4 after transfection, cells were stained using antibodies against cleaved caspase-3 (red) and Ki-67 (green). DAPI (blue), nuclear staining. Scale bar, 50 μm.

D: H1781 cells transfected with the indicated siRNA oligonucleotides were harvested by trypsinization 1 day posttransfection and seeded in soft agarose containing the indicated inhibitors alone or in combination at the same concentrations used in Figure 5C. Colonies measuring ≥50 μm were counted at day 7. Each bar represents the mean colony number ± SD of 3 wells. p values were calculated using Student's t test.

overexpressing Neu in the mammary gland develop metastatic mammary carcinomas (Guy et al., 1992). In these tumors, DNA sequence analysis revealed the presence of juxtamembrane deletions in the extracellular domain of Neu, resulting in a constitutively active receptor capable of transforming fibroblasts (Siegel et al., 1994). Such activating mutations have been reported in primary human breast cancers (Siegel et al., 1999), although their frequency remains unknown, and in two recent reports, they were not confirmed (Stephens et al., 2004, 2005). The most common change involving the proto-oncogene is mRNA overexpression with or without gene amplification (Glockner et al., 2001; Hirsch et al., 2002; Slamon et al., 1989). Recently, however, two groups reported mutations in the *HER2* gene consisting of in-frame insertions within exon 20 in NSCLC (Shigematsu et al., 2005; Stephens et al., 2004). These alterations are identical to mutations identified in the corresponding region in the *EGFR* gene in lung cancers. More recently, Lee et al. reported somatic mutations in exons 18–22 of the *HER2* kinase domain in gastric, colorectal, and breast carcinomas from Asian patients (Lee et al., 2006).

In the present report, stable expression of HER2 containing an in-frame YVMA insertion at residue 776 in nontumorigenic BEAS2B (bronchial) and MCF10A (mammary) epithelial cells was markedly more transforming than wild-type HER2. $HER2^{YVMA}$ was more potent in inducing serum-free cell proliferation, motility, and tumorigenicity in vivo as well as preventing apoptosis compared to $HER2^{WT}$. In addition, it induced transphosphorylation of kinase-dead EGFR and exhibited higher ligand-independent tyrosine phosphorylation and stronger association with signal transducers that mediate proliferative and prosurvival responses than $HER2^{WT}$, indicating that the exon 20 insertion endows the receptor with a gain of function.

Studies with cancer cell lines and human tumors have demonstrated constitutive phosphorylation of (wild-type) HER2 (Alimandi et al., 1995; Thor et al., 2000). The biochemical basis for this constitutive activation is not clear but is consistent with the reported ability of wild-type Neu to multimerize and become activated when present in cells at high density (Samanta et al., 1994). Thus, it is generally accepted that spontaneous dimerization and activation of HER2 occurs in cancers with *HER2* gene

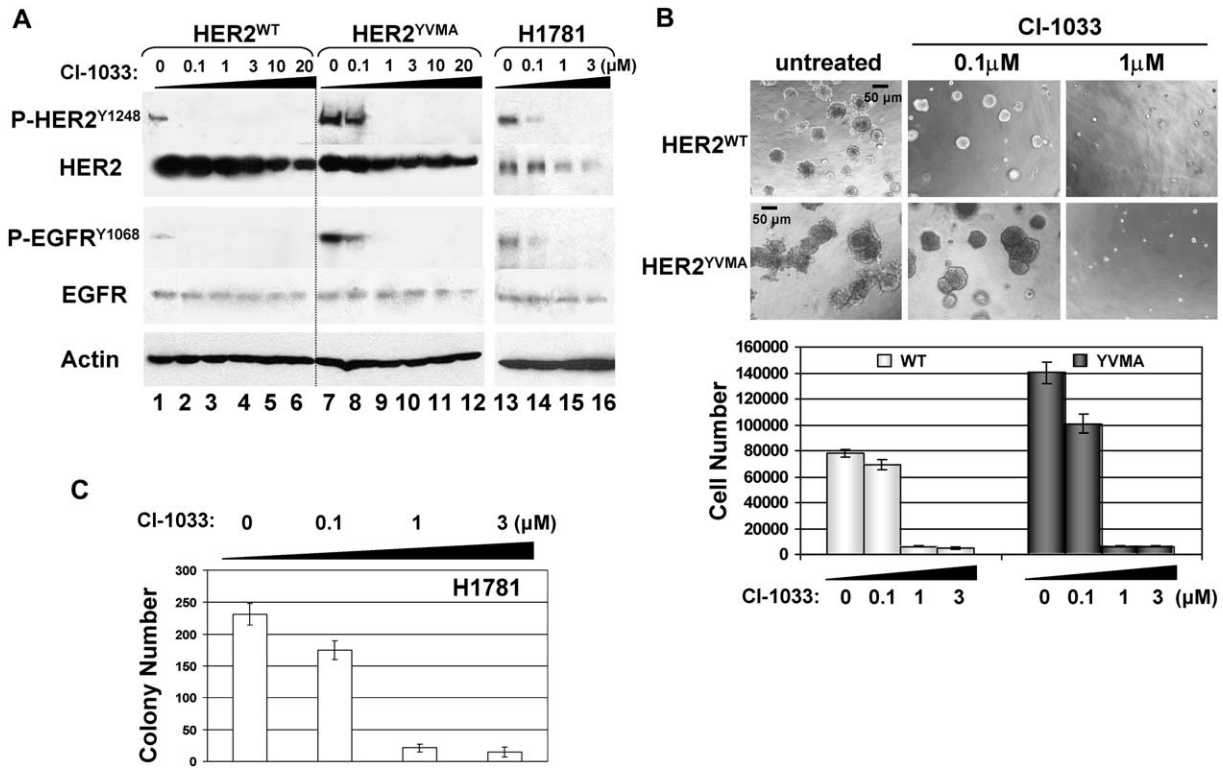

Figure 7. CI-1033 inhibits mutant HER2-driven growth and signaling

A: MCF10A cells expressing HER2^{WT} or HER2^{YVMA} and H1781 cells were treated for 16 hr with CI-1033 at the indicated concentrations. Cell lysates were prepared, separated by SDS-PAGE, and subjected to immunoblots using the indicated antibodies.

B: Top: HER2^{WT}- or HER2^{YVMA}-expressing MCF10A cells were plated on basement membrane in 8-well chambers with or without CI-1033. Inhibitors were replenished every 2 days. Phase contrast image shown was recorded 12 days after the initial seeding of cells. Scale bars, 50 μm. Bottom: 12-day acini were trypsinized, and total cell number was determined in a Coulter counter. Each bar graph represents the mean ± SD of four wells.

C: H1781 cells were seeded in soft agarose containing the indicated concentration of CI-1033. Colonies measuring ≥50 μm were counted at day 7. Each bar represents the mean colony number ± SD of three wells.

amplification. Another possible mechanism for activation of the HER2 kinase is transactivation by ligand bound EGFR or HER3/4. Indeed, coexpression of the EGFR ligand TGFα with Neu in the mammary gland of transgenic mice markedly accelerates tumor onset and progression compared to mice expressing the Neu or TGFα transgenes alone. In this study, TGFα/Neu bigenic mice exhibited increased tyrosine phosphorylation of both EGFR and Neu (Muller et al., 1996), providing evidence of EGFR-Neu crosstalk and of the ability of HER2/Neu to amplify ligand-activated EGFR signals.

On the other hand, EGFR function has been shown to be required for Neu-induced transformation. For example, EGFR TKIs can markedly delay Neu-induced tumors in transgenic mice (Lenferink et al., 2000; Lu et al., 2003). Further, MMTV/Neu mice carrying a catalytically impaired EGFR (waved-2 mice) developed breast tumors only after a prolonged latency, and the tumors that developed were fewer in number (Gillgrass et al., 2003). In MCF10A/HER2^{WT} cells, EGFR inhibition with gefitinib blocks the gain-of-function effects of transfected wild-type HER2 (Figure 5 and Ueda et al. [2004]). HER2-overexpressing cancers that also overexpress EGFR exhibit a worse outcome compared to tumors with high HER2 but undetectable EGFR (DiGiovanna et al., 2005). Finally, EGFR-positive NSCLCs that also exhibit increased (wild-type) *HER2* gene copy number respond clinically to EGFR TKIs (Cappuzzo et al., 2005; Hirsch et al., 2002), further suggesting that the EGFR is required for signaling by wild-type HER2.

In BEAS2B and MCF10A cells, HER2^{YVMA} potently induced EGFR phosphorylation. This transactivation did not require the EGFR tyrosine kinase in that it was also observed with catalytically dead K721R EGFR and was not blocked by the EGFR TKIs erlotinib and gefitinib. These results suggest that in heterodimers containing EGFR and exon 20 HER2 mutants, the EGFR tyrosine kinase activity is dispensable. EGFR function has been shown to be critical for the antiapoptotic signals generated by other oncogenes such as SOS (Sibilia et al., 2000). Therefore, it is conceivable that transactivation of the EGFR is also critical for the potent antiapoptotic effect of HER2^{YVMA}. If so, *HER2* mutations would overlap functionally with *EGFR* activating mutations, perhaps explaining the reported lack of coexistence of these alterations in primary human tumors (Lee et al., 2006; Shigematsu et al., 2005; Stephens et al., 2004).

The receptor-specific effects of EGFR and HER2 on transformation have been characterized in MCF10A mammary epithelial cells expressing chimeric EGFR or HER2 that can be homodimerized by bivalent synthetic ligands (Muthuswamy et al., 1999). In this system, activation of HER2, but not the EGFR, has been shown to reinitiate proliferation and generate 3D multiacinar MCF10A structures with a filled lumen where apoptosis is abrogated. In the study herein, HER2^{YVMA} but not HER2^{WT}

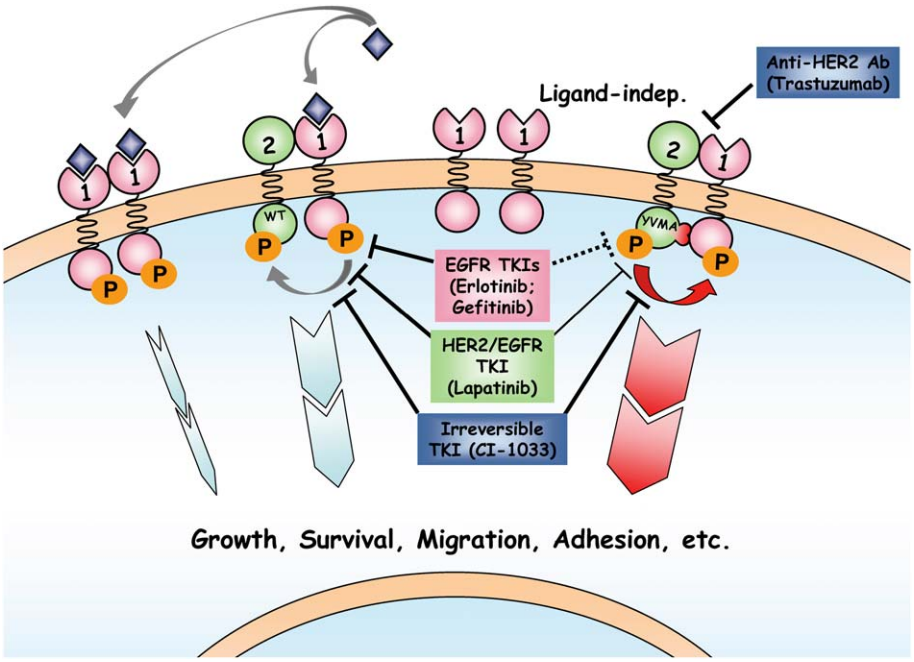

Figure 8. Schema of HER2^{YVMA} signaling output and potential response to ErbB inhibitors

Signaling by EGFR homodimers is brief and limited because of receptor endocytosis and degradation following ligand-mediated activation (Yarden and Sliwkowski, 2001) (left). Ligand-induced heterodimers of EGFR and wild-type HER2 are more stable and recruit additional cytoplasmic transducers, thus signaling with increased potency compared to EGFR homodimers (Yarden and Sliwkowski, 2001). Probably because of EGFR→HER2 transactivation, cells driven by these heterodimers are sensitive to EGFR TKIs (middle). In cells expressing the HER2 exon 20 insertion mutant, HER2 dimerizes constitutively and associates with and transactivates the EGFR. This HER2→EGFR transactivation does not require the EGFR tyrosine kinase, explaining their resistance to EGFR TKIs. Although at higher concentrations than those required to inhibit EGFR and wild-type HER2 phosphorylation, lapatinib still inhibits HER2^{YVMA} phosphorylation. Irreversible ErbB TKI CI-1033 inhibits both HER2^{WT} and HER2^{YVMA} phosphorylation. Like HER2^{WT}, the mutant receptor is partially downregulated from the cell surface by trastuzumab (right), which also inhibits cells expressing this mutation.

behaved similarly to ligand-activated chimeric ErbB2 reported by Muthuswamy et al. (2001) in the absence of AP1510, supporting the ability of the insertion mutant to potently engage antiapoptotic signals in a ligand-independent fashion. Although HER2^{WT} was also phosphorylated, it associated with Shc and p85 with lower efficiency and activated MAPK and Akt weakly compared to HER2^{YVMA}, thus potentially not reaching a threshold required for the generation of sustained survival signals.

Inhibition of mutant HER2 with RNA interference in H1781 lung cancer cells, which contain a VC insertion at G776 in exon 20 of the *HER2* gene, inhibited P-MAPK and P-Akt, reduced proliferation, and induced cell death. These cells have highly phosphorylated wild-type EGFR (Tracy et al., 2004) and are insensitive to gefitinib and erlotinib (Figure 6). Of note, a similar insertion is exon 20 of the EGFR is also resistant to these EGFR TKIs (Greulich et al., 2005). However, direct inhibitors of HER2 such as trastuzumab, lapatinib, and CI-1033 reduced colony formation by MCF10A/HER2^{YVMA} and H1781 cells. In MCF10/HER2^{YVMA} cells, treatment with trastuzumab downregulated mutant HER2 from the cell surface, while lapatinib and CI-1033 inhibited HER2 phosphorylation, further suggesting that cancers expressing this mutant remain HER2 dependent and thus sensitive to HER2-targeted therapies. Clinical data to support this possibility are not available, since there are no published trials with single-agent trastuzumab or lapatinib in NSCLC, where a low frequency of *HER2* mutations has been reported. Thus, the therapeutic efficacy of anti-HER2 strategies in this patient population requires prospective investigation.

Finally, and based on the results with MCF10A and H1781 cells treated with erlotinib and gefitinib, we propose, first, that EGFR inhibitors would be effective against tumors driven by heterodimers of EGFR and wild-type HER2. In these cancers, HER2 amplifies signals by EGFR/HER2 heterodimers, which remain dependent on the EGFR kinase (Figure 8). This possibility is supported by a recent report in which EGFR-positive NSCLCs with wild-type *HER2* gene amplification responded clinically to EGFR TKI gefitinib (Cappuzzo et al., 2005). In a recent randomized survival study of erlotinib versus best supportive care in NSCLC patients (Shepherd et al., 2005), this correlation with clinical response remains to be investigated. Second, we predict that cancers expressing mutation/insertions in exon 20 of *HER2* would be insensitive to small molecule inhibitors of the EGFR tyrosine kinase. Indeed, in a very recent study from Korea, all four patients with lung adenocarcinoma containing HER2 mutations progressed on gefitinib. Three of the four contained mutations in exon 20 (Han et al., 2006). Third, in these cancers, a combination of trastuzumab and lapatinib or the irreversible HER2 inhibitor CI-1033 may have clinical activity and is worthy of prospective investigation.

Experimental procedures

Cell lines, plasmids, and viruses

All cells were from the American Type Culture Collection (ATCC). Cell culture, plasmid cloning, and retroviral transduction were carried out according to standard procedures (details provided in Supplemental Data). The following reagents were used: human TGFα and EGF (Calbiochem), puromycin (Calbiochem), G418 (Research Products International Corp.), erlotinib (from Mark Sliwkowski, Genentech), gefitinib (from Alan Wakeling, AstraZeneca Pharmaceuticals), lapatinib (from Tona Gilmer, GlaxoSmithKline), and CI-1033 (from David Fry, Parke-Davis). Trastuzumab was purchased at the Vanderbilt University Medical Center Pharmacy. The EGFR^{K721R}-GFP plasmid was kindly provided by Brent Polk (Vanderbilt University).

Immunoprecipitation and immunoblot analysis

Immunoprecipitation and immunoblot analysis were performed using standard protocols (details provided in Supplemental Data).

Cell growth, apoptosis, and motility assays

Equal numbers of cells were seeded on 12-well plates and allowed to grow in full medium. Cells were harvested by trypsinization every 24 hr, and cell number was determined in a Coulter counter. Cells growing on 100 mm dishes were serum starved for 3 days and collected for apoptosis assay using an Apo-BrdU kit (Phoenix Flow Systems, Inc.) according to the manufacturer's

protocol. FITC-positive apoptotic cells were quantitated in a FACS/Calibur Flow Cytometer (BD Biosciences).

For wound closure assays, cells were allowed to reach confluence on a 6-well plate and then serum starved for 24 hr. The monolayers were scraped with a plastic pipette tip and replenished with fresh serum-free medium. Phase contrast images were photographed at 0, 10, and 24 hr after wounding. Transwell motility assays were performed utilizing 5 μm pore, 6.5 mm polycarbonate transwell filters (Corning Costar Corp.). Cells (1.5×10^5 per well) were seeded in serum-free medium onto the upper surface of the filters and allowed to migrate. After 24 hr, the cells on the upper surface of the filters were wiped off with a cotton swab. Cells that had migrated to the filter underside were fixed, stained with Diff-Quik stain set (Dade Behring, Inc.), and counted by bright field microscopy.

Soft agarose colony-forming assay

Base layers consisting of growth medium containing 0.8% low-melting point agarose (Gibco) and 10 mM HEPES (pH 7.5) were poured onto 6-well plates and allowed to solidify. Cells (3×10^4 per well) were plated in triplicate in top layers consisting of growth medium containing 0.4% agarose and 5 mM HEPES. Colonies measuring $\geq$50 μm were photographed after 7–10 days and counted manually.

Xenograft studies

Exponentially growing cells on 150 mm dishes were scraped off and resuspended in serum-free medium; 2×10^6 cells in 0.3 ml were then injected subcutaneously via a 22-gauge needle into each of 4-week-old female athymic nude mice (Harlan Sprague-Dawley). Tumor formation was monitored by palpation twice a week. Volume of tumors measuring $\geq$3 mm in diameter was calculated by the formula: volume = width^2 × length/2. These experiments were approved by the Vanderbilt Institutional Animal Care Committee and performed under institutional guidelines in accordance with approved regulatory standards.

Three-dimensional morphogenesis and indirect immunofluorescence

MCF10A cells expressing HER2^{WT}, HER2^{YVMA}, or vector were seeded on Growth Factor Reduced Matrigel (BD Biosciences) in 8-well chamber slides following the protocol described by Debnath et al. (2003) Morphogenesis of acini was photographed every 2 days. For cell number counting, cultures growing on Matrigel were trypsinized and cell numbers were measured in a Coulter counter. Invasion assay was performed in BD BioCoat Growth Factor Reduced Matrigel invasion chambers (BD Biosciences) according to the manufacturer's protocol. Immunofluorescence staining of 3D acini was performed as described by Debnath et al. (2003) using antibodies against β-catenin (BD Biosciences), cleaved caspase-3 (Cell Signaling), Ki-67 (Calbiochem), and Myc tag. Confocal analyses were performed with Zeiss inverted LSM510 confocal microscopy system. Indirect immunofluorescence assay (IFA) was performed as described previously (Wang et al., 2005). Fluorescent images were captured using a Princeton Instruments cooled CCD digital camera from a Zeiss Axiophot upright microscope. Primary antibodies include Ki-67 and cleaved caspase-3. The fluorescent antibodies are Oregon green-α-mouse IgG and Texas red-α-rabbit IgG (Molecular Probes).

Transfection of DNA and siRNA, total RNA extraction, and RT-PCR

Cell transfection, RNA extraction, and RT-PCR were performed using standard protocols (details provided in Supplemental Data).

Cell surface biotinylation

Cells plated in 100 mm dishes were treated or not with trastuzumab (10 μg/ml) for 24 hr at 37°C and washed with PBS. Bound antibody was removed by incubating cells for 6 min on ice with cold acid wash buffer (0.5 M NaCl, 0.2 M sodium acetate [pH 3.0]). After three washes with cold PBS (pH 8.0), cells were incubated with freshly prepared Sulfo-NHS-Biotin reagent (2 mM; Pierce) for 30 min at 4°C. The reaction was quenched with 100 mM glycine in PBS, and the cells were lysed in NP-40 buffer. Equal amounts of protein extracts (500 μg) were subjected to precipitation using Streptavidin Magnetic Spheres (Promega) followed by SDS-PAGE and HER2 immunoblot.

In vitro kinase assays

Five hundred micrograms of total protein extracted from MCF10A/HER2^{WT} or MCF10A/HER2^{YVMA} cells were immunoprecipitated with a Myc tag antibody. The precipitates were washed twice in NP-40 lysis buffer, twice in kinase buffer (20 mM HEPES [pH 7.5], 10 mM $MgCl_2$, 10 mM $MnCl_2$, 1 mM dithiothreitol, 0.1 mM Na_3VO_4), and then aliquoted on ice into two equal portions, each brought up to a final volume of 40 μl by adding kinase buffer. ATP was added to one aliquot (final concentration 0.1 mM) but not to the other aliquot. The kinase reaction was allowed to proceed for 5 min at 30°C and then terminated by adding 5× loading buffer and boiling for 3 min before separation by 7.5% SDS-PAGE followed by immunoblot analysis. In the reaction using kinase-dead EGFR as substrate, the EGFR^{K721R}-GFP plasmid was transiently expressed by 32D cells followed by precipitation using a GFP antibody. Precipitated EGFR^{K721R}-GFP was incubated with HER2^{WT}, HER2^{YVMA} receptors, or control precipitates in the absence or presence of 0.1 mM ATP. A kinase reaction was carried out under the same conditions as above, and its products were resolved by 7.5% SDS-PAGE and visualized by P-Tyr, EGFR, and Myc immunoblot analyses.

Supplemental data

The Supplemental Data include Supplemental Experimental Procedures and four supplemental figures and can be found with this article online at http://www.cancercell.org/cgi/content/full/10/1/25/DC1/.

Acknowledgments

This work was supported by NCI R01 CA62212 (C.L.A.), R01 CA80195 (C.L.A.), Breast Cancer Specialized Program of Research Excellence (SPORE) grant P50 CA98131, Lung Cancer SPORE grant P50 CA90949, and Vanderbilt-Ingram Comprehensive Cancer Center Support Grant P30 CA68485. M.P.-T. is supported by NCI T32 CA78136.

Received: April 13, 2006
Revised: May 13, 2006
Accepted: May 31, 2006
Published: July 17, 2006

References

Agus, D.B., Akita, R.W., Fox, W.D., Lewis, G.D., Higgins, B., Pisacane, P.I., Lofgren, J.A., Tindell, C., Evans, D.P., Maiese, K., et al. (2002). Targeting ligand-activated ErbB2 signaling inhibits breast and prostate tumor growth. Cancer Cell *2*, 127–137.

Alimandi, M., Romano, A., Curia, M.C., Muraro, R., Fedi, P., Aaronson, S.A., Di Fiore, P.P., and Kraus, M.H. (1995). Cooperative signaling of ErbB3 and ErbB2 in neoplastic transformation and human mammary carcinomas. Oncogene *10*, 1813–1821.

Biscardi, J.S., Maa, M.C., Tice, D.A., Cox, M.E., Leu, T.H., and Parsons, S.J. (1999). c-Src-mediated phosphorylation of the epidermal growth factor receptor on Tyr845 and Tyr1101 is associated with modulation of receptor function. J. Biol. Chem. *274*, 8335–8343.

Cappuzzo, F., Varella-Garcia, M., Shigematsu, H., Domenichini, I., Bartolini, S., Ceresoli, G.L., Rossi, E., Ludovini, V., Gregorc, V., Toschi, L., et al. (2005). Increased HER2 gene copy number is associated with response to gefitinib therapy in epidermal growth factor receptor-positive non-small-cell lung cancer patients. J. Clin. Oncol. *23*, 5007–5018.

Citri, A., Alroy, I., Lavi, S., Rubin, C., Xu, W., Grammatikakis, N., Patterson, C., Neckers, L., Fry, D.W., and Yarden, Y. (2002). Drug-induced ubiquitylation and degradation of ErbB receptor tyrosine kinases: implications for cancer therapy. EMBO J. *21*, 2407–2417.

Debnath, J., and Brugge, J.S. (2005). Modelling glandular epithelial cancers in three-dimensional cultures. Nat. Rev. Cancer *5*, 675–688.

Debnath, J., Mills, K.R., Collins, N.L., Reginato, M.J., Muthuswamy, S.K., and Brugge, J.S. (2002). The role of apoptosis in creating and maintaining luminal space within normal and oncogene-expressing mammary acini. Cell *111*, 29–40.

Debnath, J., Muthuswamy, S.K., and Brugge, J.S. (2003). Morphogenesis and oncogenesis of MCF-10A mammary epithelial acini grown in three-dimensional basement membrane cultures. Methods *30*, 256–268.

DiGiovanna, M.P., and Stern, D.F. (1995). Activation state-specific monoclonal antibody detects tyrosine phosphorylated p185neu/erbB-2 in a subset of human breast tumors overexpressing this receptor. Cancer Res. *55*, 1946–1955.

DiGiovanna, M.P., Stern, D.F., Edgerton, S.M., Whalen, S.G., Moore, D., II, and Thor, A.D. (2005). Relationship of epidermal growth factor receptor expression to ErbB-2 signaling activity and prognosis in breast cancer patients. J. Clin. Oncol. *23*, 1152–1160.

Ewald, J.A., Wilkinson, J.C., Guyer, C.A., and Staros, J.V. (2003). Ligand- and kinase activity-independent cell survival mediated by the epidermal growth factor receptor expressed in 32D cells. Exp. Cell Res. *282*, 121–131.

Gazdar, A.F., Shigematsu, H., Herz, J., and Minna, J.D. (2004). Mutations and addiction to EGFR: the Achilles 'heal' of lung cancers? Trends Mol. Med. *10*, 481–486.

Gillgrass, A., Cardiff, R.D., Sharan, N., Kannan, S., and Muller, W.J. (2003). Epidermal growth factor receptor-dependent activation of Gab1 is involved in ErbB-2-mediated mammary tumor progression. Oncogene *22*, 9151–9155.

Glockner, S., Lehmann, U., Wilke, N., Kleeberger, W., Langer, F., and Kreipe, H. (2001). Amplification of growth regulatory genes in intraductal breast cancer is associated with higher nuclear grade but not with the progression to invasiveness. Lab. Invest. *81*, 565–571.

Graus-Porta, D., Beerli, R.R., Daly, J.M., and Hynes, N.E. (1997). ErbB-2, the preferred heterodimerization partner of all ErbB receptors, is a mediator of lateral signaling. EMBO J. *16*, 1647–1655.

Greulich, H., Chen, T.H., Feng, W., Janne, P.A., Alvarez, J.V., Zappaterra, M., Bulmer, S.E., Frank, D.A., Hahn, W.C., Sellers, W.R., and Meyerson, M. (2005). Oncogenic transformation by inhibitor-sensitive and -resistant EGFR mutants. PLoS Med *2*, e313. 10.1371/journal.pmed.0020313.

Guy, C.T., Webster, M.A., Schaller, M., Parsons, T.J., Cardiff, R.D., and Muller, W.J. (1992). Expression of the neu protooncogene in the mammary epithelium of transgenic mice induces metastatic disease. Proc. Natl. Acad. Sci. USA *89*, 10578–10582.

Han, S.W., Kim, T.Y., Jeon, Y.K., Hwang, P.G., Im, S.A., Lee, K.H., Kim, J.H., Kim, D.W., Heo, D.S., Kim, N.K., et al. (2006). Optimization of patient selection for gefitinib in non-small cell lung cancer by combined analysis of epidermal growth factor receptor mutation, K-ras mutation, and Akt phosphorylation. Clin. Cancer Res. *12*, 2538–2544.

Hernan, R., Fasheh, R., Calabrese, C., Frank, A.J., Maclean, K.H., Allard, D., Barraclough, R., and Gilbertson, R.J. (2003). ERBB2 up-regulates S100A4 and several other prometastatic genes in medulloblastoma. Cancer Res. *63*, 140–148.

Hirsch, F.R., Varella-Garcia, M., Franklin, W.A., Veve, R., Chen, L., Helfrich, B., Zeng, C., Baron, A., and Bunn, P.A., Jr. (2002). Evaluation of HER-2/neu gene amplification and protein expression in non-small cell lung carcinomas. Br. J. Cancer *86*, 1449–1456.

Lee, J.W., Soung, Y.H., Seo, S.H., Kim, S.Y., Park, C.H., Wang, Y.P., Park, K., Nam, S.W., Park, W.S., Kim, S.H., et al. (2006). Somatic mutations of ERBB2 kinase domain in gastric, colorectal, and breast carcinomas. Clin. Cancer Res. *12*, 57–61.

Lenferink, A.E., Simpson, J.F., Shawver, L.K., Coffey, R.J., Forbes, J.T., and Arteaga, C.L. (2000). Blockade of the epidermal growth factor receptor tyrosine kinase suppresses tumorigenesis in MMTV/Neu + MMTV/TGF-α bigenic mice. Proc. Natl. Acad. Sci. USA *97*, 9609–9614.

Lu, C., Speers, C., Zhang, Y., Xu, X., Hill, J., Steinbis, E., Celestino, J., Shen, Q., Kim, H., Hilsenbeck, S., et al. (2003). Effect of epidermal growth factor receptor inhibitor on development of estrogen receptor-negative mammary tumors. J. Natl. Cancer Inst. *95*, 1825–1833.

Moasser, M.M., Basso, A., Averbuch, S.D., and Rosen, N. (2001). The tyrosine kinase inhibitor ZD1839 ("Iressa") inhibits HER2-driven signaling and suppresses the growth of HER2-overexpressing tumor cells. Cancer Res. *61*, 7184–7188.

Moulder, S.L., Yakes, F.M., Muthuswamy, S.K., Bianco, R., Simpson, J.F., and Arteaga, C.L. (2001). Epidermal growth factor receptor (HER1) tyrosine kinase inhibitor (Iressa) inhibits HER2/neu (erbB2)-overexpressing breast cancer cells in vitro and in vivo. Cancer Res. *61*, 8887–8895.

Muller, W.J., Arteaga, C.L., Muthuswamy, S.K., Siegel, P.M., Webster, M.A., Cardiff, R.D., Meise, K.S., Li, F., Halter, S.A., and Coffey, R.J. (1996). Synergistic interaction of the Neu proto-oncogene product and transforming growth factor α in the mammary epithelium of transgenic mice. Mol. Cell. Biol. *16*, 5726–5736.

Muthuswamy, S.K., Gilman, M., and Brugge, J.S. (1999). Controlled dimerization of ErbB receptors provides evidence for differential signaling by homo- and heterodimers. Mol. Cell. Biol. *19*, 6845–6857.

Muthuswamy, S.K., Li, D., Lelievre, S., Bissell, M.J., and Brugge, J.S. (2001). ErbB2, but not ErbB1, reinitiates proliferation and induces luminal repopulation in epithelial acini. Nat. Cell Biol. *3*, 785–792.

Pierce, J.H., Ruggiero, M., Fleming, T.P., Di Fiore, P.P., Greenberger, J.S., Varticovski, L., Schlessinger, J., Rovera, G., and Aaronson, S.A. (1988). Signal transduction through the EGF receptor transfected in IL-3-dependent hematopoietic cells. Science *239*, 628–631.

Pierce, J.H., Arnstein, P., DiMarco, E., Artrip, J., Kraus, M.H., Lonardo, F., Di Fiore, P.P., and Aaronson, S.A. (1991). Oncogenic potential of erbB-2 in human mammary epithelial cells. Oncogene *6*, 1189–1194.

Pinkas-Kramarski, R., Soussan, L., Waterman, H., Levkowitz, G., Alroy, I., Klapper, L., Lavi, S., Seger, R., Ratzkin, B.J., Sela, M., and Yarden, Y. (1996). Diversification of Neu differentiation factor and epidermal growth factor signaling by combinatorial receptor interactions. EMBO J. *15*, 2452–2467.

Rusnak, D.W., Affleck, K., Cockerill, S.G., Stubberfield, C., Harris, R., Page, M., Smith, K.J., Guntrip, S.B., Carter, M.C., Shaw, R.J., et al. (2001). The characterization of novel, dual ErbB-2/EGFR, tyrosine kinase inhibitors: potential therapy for cancer. Cancer Res. *61*, 7196–7203.

Samanta, A., LeVea, C.M., Dougall, W.C., Qian, X., and Greene, M.I. (1994). Ligand and p185c-neu density govern receptor interactions and tyrosine kinase activation. Proc. Natl. Acad. Sci. USA *91*, 1711–1715.

Shepherd, F.A., Rodrigues Pereira, J., Ciuleanu, T., Tan, E.H., Hirsh, V., Thongprasert, S., Campos, D., Maoleekoonpiroj, S., Smylie, M., Martins, R., et al. (2005). Erlotinib in previously treated non-small-cell lung cancer. N. Engl. J. Med. *353*, 123–132.

Shigematsu, H., Takahashi, T., Nomura, M., Majmudar, K., Suzuki, M., Lee, H., Wistuba, I.I., Fong, K.M., Toyooka, S., Shimizu, N., et al. (2005). Somatic mutations of the HER2 kinase domain in lung adenocarcinomas. Cancer Res. *65*, 1642–1646.

Sibilia, M., Fleischmann, A., Behrens, A., Stingl, L., Carroll, J., Watt, F.M., Schlessinger, J., and Wagner, E.F. (2000). The EGF receptor provides an essential survival signal for SOS-dependent skin tumor development. Cell *102*, 211–220.

Siegel, P.M., Dankort, D.L., Hardy, W.R., and Muller, W.J. (1994). Novel activating mutations in the neu proto-oncogene involved in induction of mammary tumors. Mol. Cell. Biol. *14*, 7068–7077.

Siegel, P.M., Ryan, E.D., Cardiff, R.D., and Muller, W.J. (1999). Elevated expression of activated forms of Neu/ErbB-2 and ErbB-3 are involved in the induction of mammary tumors in transgenic mice: implications for human breast cancer. EMBO J. *18*, 2149–2164.

Slamon, D.J., Godolphin, W., Jones, L.A., Holt, J.A., Wong, S.G., Keith, D.E., Levin, W.J., Stuart, S.G., Udove, J., Ullrich, A., et al. (1989). Studies of the HER-2/neu proto-oncogene in human breast and ovarian cancer. Science *244*, 707–712.

Slamon, D.J., Leyland-Jones, B., Shak, S., Fuchs, H., Paton, V., Bajamonde, A., Fleming, T., Eiermann, W., Wolter, J., Pegram, M., et al. (2001). Use of chemotherapy plus a monoclonal antibody against HER2 for metastatic breast cancer that overexpresses HER2. N. Engl. J. Med. *344*, 783–792.

Smaill, J.B., Rewcastle, G.W., Loo, J.A., Greis, K.D., Chan, O.H., Reyner, E.L., Lipka, E., Showalter, H.D., Vincent, P.W., Elliott, W.L., and Denny, W.A. (2000). Tyrosine kinase inhibitors. 17. Irreversible inhibitors of the epidermal growth factor receptor: 4-(phenylamino)quinazoline- and 4-(phenylamino)pyrido. J. Med. Chem. *43*, 1380–1397.

Stephens, P., Hunter, C., Bignell, G., Edkins, S., Davies, H., Teague, J., Stevens, C., O'Meara, S., Smith, R., Parker, A., et al. (2004). Lung cancer: intragenic ERBB2 kinase mutations in tumours. Nature *431*, 525–526.

Stephens, P., Edkins, S., Davies, H., Greenman, C., Cox, C., Hunter, C., Bignell, G., Teague, J., Smith, R., Stevens, C., et al. (2005). A screen of the complete protein kinase gene family identifies diverse patterns of somatic mutations in human breast cancer. Nat. Genet. *37*, 590–592.

Stover, D.R., Becker, M., Liebetanz, J., and Lydon, N.B. (1995). Src phosphorylation of the epidermal growth factor receptor at novel sites mediates receptor interaction with Src and P85 α. J. Biol. Chem. *270*, 15591–15597.

Thor, A.D., Liu, S., Edgerton, S., Moore, D., 2nd, Kasowitz, K.M., Benz, C.C., Stern, D.F., and DiGiovanna, M.P. (2000). Activation (tyrosine phosphorylation) of ErbB-2 (HER-2/neu): a study of incidence and correlation with outcome in breast cancer. J. Clin. Oncol. *18*, 3230–3239.

Tracy, S., Mukohara, T., Hansen, M., Meyerson, M., Johnson, B.E., and Janne, P.A. (2004). Gefitinib induces apoptosis in the EGFRL858R non-small-cell lung cancer cell line H3255. Cancer Res. *64*, 7241–7244.

Ueda, Y., Wang, S., Dumont, N., Yi, J.Y., Koh, Y., and Arteaga, C.L. (2004). Overexpression of HER2 (erbB2) in human breast epithelial cells unmasks transforming growth factor β-induced cell motility. J. Biol. Chem. *279*, 24505–24513.

Vogel, C.L., Cobleigh, M.A., Tripathy, D., Gutheil, J.C., Harris, L.N., Fehrenbacher, L., Slamon, D.J., Murphy, M., Novotny, W.F., Burchmore, M., et al. (2002). Efficacy and safety of trastuzumab as a single agent in first-line treatment of HER2-overexpressing metastatic breast cancer. J. Clin. Oncol. *20*, 719–726.

Wang, L.M., Kuo, A., Alimandi, M., Veri, M.C., Lee, C.C., Kapoor, V., Ellmore, N., Chen, X.H., and Pierce, J.H. (1998). ErbB2 expression increases the spectrum and potency of ligand-mediated signal transduction through ErbB4. Proc. Natl. Acad. Sci. USA *95*, 6809–6814.

Wang, S.E., Wu, F.Y., Shin, I., Qu, S., and Arteaga, C.L. (2005). Transforming growth factor β (TGF-β)-Smad target gene protein tyrosine phosphatase receptor type kappa is required for TGF-β function. Mol. Cell. Biol. *25*, 4703–4715.

Worthylake, R., Opresko, L.K., and Wiley, H.S. (1999). ErbB-2 amplification inhibits down-regulation and induces constitutive activation of both ErbB-2 and epidermal growth factor receptors. J. Biol. Chem. *274*, 8865–8874.

Yarden, Y., and Sliwkowski, M.X. (2001). Untangling the ErbB signalling network. Nat. Rev. Mol. Cell Biol. *2*, 127–137.

Ye, D., Mendelsohn, J., and Fan, Z. (1999). Augmentation of a humanized anti-HER2 mAb 4D5 induced growth inhibition by a human-mouse chimeric anti-EGF receptor mAb C225. Oncogene *18*, 731–738.

Zhang, K., Sun, J., Liu, N., Wen, D., Chang, D., Thomason, A., and Yoshinaga, S.K. (1996). Transformation of NIH 3T3 cells by HER3 or HER4 receptors requires the presence of HER1 or HER2. J. Biol. Chem. *271*, 3884–3890.